HHS Public Access

Author manuscript

Lancet Infect Dis. Author manuscript; available in PMC 2024 June 02.

Published in final edited form as:

Lancet Infect Dis. 2019 September ; 19(9): 1023–1032. doi:10.1016/S1473-3099(19)30291-9.

Characterisation of infectious Ebola virus from the ongoing outbreak to guide response activities in the Democratic Republic of the Congo: a phylogenetic and in vitro analysis

Laura K McMullan,
Viral Special Pathogens Branch, Division of High-Consequence Pathogens and Pathology, National Center for Emerging and Zoonotic Infectious Diseases, Centers for Disease Control and Prevention, Atlanta, GA, USA

Mike Flint,
Viral Special Pathogens Branch, Division of High-Consequence Pathogens and Pathology, National Center for Emerging and Zoonotic Infectious Diseases, Centers for Disease Control and Prevention, Atlanta, GA, USA

Ayan Chakrabarti,
Viral Special Pathogens Branch, Division of High-Consequence Pathogens and Pathology, National Center for Emerging and Zoonotic Infectious Diseases, Centers for Disease Control and Prevention, Atlanta, GA, USA

Lisa Guerrero,
Viral Special Pathogens Branch, Division of High-Consequence Pathogens and Pathology, National Center for Emerging and Zoonotic Infectious Diseases, Centers for Disease Control and Prevention, Atlanta, GA, USA

Michael K Lo,
Viral Special Pathogens Branch, Division of High-Consequence Pathogens and Pathology, National Center for Emerging and Zoonotic Infectious Diseases, Centers for Disease Control and Prevention, Atlanta, GA, USA

Danielle Porter,
Gilead Sciences, Foster City, CA, USA

Stuart TNichol,
Viral Special Pathogens Branch, Division of High-Consequence Pathogens and Pathology, National Center for Emerging and Zoonotic Infectious Diseases, Centers for Disease Control and Prevention, Atlanta, GA, USA

Correspondence to: Dr Laura K McMullan, Viral Special Pathogens Branch, Division of High-Consequence Pathogens and Pathology, National Center for Emerging and Zoonotic Infectious Diseases, Centers for Disease Control and Prevention, Atlanta, GA 30329, USA, lim8@cdc.gov.

Contributors

LKM and CA conceived and designed the experiments. LKM, AC, LG, and CA did the experiments and collected data. MKL and DP provided reagents. CFS, STN, and CA provided supervision. LKM and MF wrote the manuscript, and LKM, MF, DP, STN, and CA reviewed and edited the final versions.

Declaration of interests

Danielle Porter is an employee of Gilead Sciences. All other authors declare no competing interests.

Christina F Spiropoulou,
Viral Special Pathogens Branch, Division of High-Consequence Pathogens and Pathology, National Center for Emerging and Zoonotic Infectious Diseases, Centers for Disease Control and Prevention, Atlanta, GA, USA

Cesar Albarino
Viral Special Pathogens Branch, Division of High-Consequence Pathogens and Pathology, National Center for Emerging and Zoonotic Infectious Diseases, Centers for Disease Control and Prevention, Atlanta, GA, USA

Summary

Background—The ongoing Ebola virus outbreak in the Ituri and North Kivu Provinces of the Democratic Republic of the Congo, which began in July, 2018, is the second largest ever recorded. Despite civil unrest, outbreak control measures and the administration of experimental therapies and a vaccine have been initiated. The aim of this study was to test the efficacy of candidate therapies and diagnostic tests with the outbreak strain Ituri Ebola virus. Lacking a virus isolate from this outbreak, a recombinant Ituri Ebola virus was compared with a similarly engineered Makona virus from the 2013–16 outbreak.

Methods—Using Ebola virus sequences provided by organisations in DR Congo and a reverse genetics system, we generated an authentic Ebola virus from the ongoing outbreak in Ituri and North Kivu provinces. To relate this virus to other Ebola viruses in DR Congo, we did a phylogenetic analysis of representative complete Ebola virus genome sequences from previous outbreaks. We evaluated experimental therapies being tested in clinical trials in DR Congo, including remdesivir and ZMapp monoclonal antibodies, for their ability to inhibit the growth of infectious Ituri Ebola virus in cell culture. We also tested diagnostic assays for detection of the Ituri Ebola virus sequence.

Findings—The phylogenetic analysis of whole-genome sequences from each Ebola virus outbreak suggests there are at least two Ebola virus strains in DR Congo, which have independently crossed into the human population. The Ituri Ebola strain initially grew slower than the Makona strain, yet reached similar mean yields of 3×10^7 50% tissue culture infectious dose by 72 h infection in Huh-7 cells. Ituri Ebola virus was similar to Makona in its susceptibility to inhibition by remdesivir and to neutralisation by monoclonal antibodies from ZMapp and other monoclonal antibodies. Remdesivir inhibited Ituri Ebola virus at a 50% effective concentration (EC_{50}) of 12nM (with a selectivity index of 303) and Makona Ebola virus at 13nM (with a selectivity index of 279). The Zmapp monoclonal antibodies 2G4 and 4G7 neutralised Ituri Ebola virus with a mean EC_{50} of 0·24 μg/mL and 0·48 μg/mL, and Makona Ebola virus with a mean EC_{50} of 0·45 μg/mL and 0·2 μg/mL. The Xpert Ebola and US Centers for Disease Control and Prevention real-time RT-qPCR diagnostic assays detected Ituri and Makona Ebola virus sequences with similar sensitivities and efficiencies, despite primer site binding mismatches in the Ituri Ebola virus.

Interpretation—Our findings provide a rationale for the continued testing of investigational therapies, confirm the effectiveness of the diagnostic assays used in the region, and establish a paradigm for the use of reverse genetics to inform response activities in an outbreak.

Funding—US Centers for Disease Control and Prevention.

Introduction

Viruses of the genus Ebolavirus cause sporadic outbreaks of severe haemorrhagic fever, with case fatality of up to 90%.[1] On July 30, 2018, the Ministry of Health of the Democratic Republic of the Congo declared their tenth outbreak of Ebola virus disease, in the Mabalako health district in North Kivu. This was just weeks after declaring the end of the ninth outbreak in the western town of Bikoro, Équateur Province, 780 miles away. Responding to any filovirus outbreak is challenging and requires a combination of clinical, laboratory, and epidemiological approaches to halt virus transmission. Community engagement and education are key to enabling contact tracing and safe and dignified burials. The mineral-rich area of eastern DR Congo is experiencing a humanitarian crisis that has lasted more than a decade, hampering response activities. Despite best efforts of the Ministry of Health, Médecins Sans Frontières, WHO, and many other organisations, the ongoing outbreak in the Ituri and North Kivu provinces is now the second largest and longest Ebola virus (EBOV) outbreak ever recorded, with 2181 cases and 1459 deaths (as of June 17, 2019).[2]

In DR Congo, an extensive immunisation campaign with the experimental vaccine rVSV-ZEBOV is underway, but effective treatments for Ebola virus disease are urgently needed. In North Kivu, a randomised clinical trial (registered with ClinicalTrials.gov, number NCT03719586) has been initiated to compare mortality among patients receiving four different investi-gational EBOV therapies: mono-clonal antibody cocktails ZMapp (developed by Mapp Biopharmaceuticals, San Diego, CA, USA) and REGN-EB3 (developed by Regeneron Pharmaceuticals, Eastview, NY, USA), single monoclonal antibody mAb114 (developed by the National Institutes of Health, Bethesda, MD, USA), and the small molecule remdesivir (also known as GS-5734, developed by Gilead Sciences, Foster City, CA, USA). The monoclonal antibodies bind to the EBOV glycoprotein (GP) to neutralise the virus, while remdesivir is a nucleotide analogue prodrug that inhibits the viral polymerase.[3]

Despite security concerns in the area, scientists with the Institut National de Recherche Biomédicale (INRB; Kinshasa, Democratic Republic of the Congo) and the United States Army Medical Research Institute of Infectious Diseases (USAMRIID; Fort Detrick, MD, USA) established a sequencing facility in DR Congo in May, 2018. They succeeded in generating high-quality, accurate sequences from the Ituri-North Kivu outbreak, which they shared with the scientific community. Their work allowed the early identification of Zaire EBOV as the causative agent of the outbreak. In partnership with local and international collaborators, analyses of these outbreak sequences elucidated early transmission chains and identified the index case to be from the Mangina health district.[4]

Because of the containment requirements, surrogate assays and in silico analyses are often used to predict biological activities for EBOV. Although these can be informative, we sought to provide a more definitive evaluation of candidate therapies and diagnostic assays by testing them using infectious EBOV-Ituri. Lacking an isolate from this outbreak, the aim of this study was to rescue recombinant, infectious EBOV-Ituri from plasmid DNA, and to

use this virus for our evaluations. The International Committee on Taxonomy of Viruses has established guidelines[5] for Ebola nomenclature and declared EBOV to indicate the Ebola Zaire species only. Ituri is a variant of the Ebola Zaire species; we have referred to other Ebola virus species by name (eg, Bundibugyo).

Methods

Study design

This study was designed to generate infectious EBOV-Ituri with which to evaluate candidate antiviral therapies and existing diagnostic tests. We generated a recombinant virus expressing a reporter protein, Zoanthus green fluorescent protein (ZsG), such that virus growth was quantifiable by measuring fluorescence in infected cells. Growth and inhibition of EBOV-Ituri was compared with that of similarly engineered EBOV-Makona. In compliance with US Centers for Disease Control and Prevention (CDC) policy, this study was reviewed and approved by the CDC Institutional Biosafety Committee before its initiation, and it is reported in accordance with the US Government Policy for Oversight of Life Sciences Dual Use Research of Concern.

Cells, viruses, and antibodies

Human hepatocellular carcinoma Huh-7 cells (Apath, New York, NY, USA) were cultured in Dulbecco's modified Eagle medium (DMEM) supplemented with 1× nonessential amino acids and 10% fetal calf serum (FCS) at 37°C in 5% CO_2. The EBOV-Makona-ZsGreen1 reporter virus expressing ZsG was generated as described previously.[6] Monoclonal antibodies 13F6 (0201–022), c13C6 (0201–023), c6D8 (0201–021), 4F3 (0201–020), and KZ52 (0260–001) were from IBT Bioservices (Rockville, MD, USA). The ZMapp prototype monoclonal antibodies 4G7 and 2G4 were donated by Gary Kobinger (Infectious Disease Research Center, Laval University, Quebec City, QC, Canada). Unlabelled IgG controls were obtained from Southern Biotech (Birmingham, AL, USA). Antibodies derived from convalescent patients were donated by Carl Davis and Rafi Ahmed (Emory University, Atlanta, GA, USA).

Phylogenetic inference of EBOV evolution

Complete genome sequences of Zaire EBOV were obtained from GenBank (appendix p 2). The EBOV genomic sequences from the Ituri-North Kivu outbreak were generously made available before publication through GenBank, by INRB-USAMRIID scientists. Full-length EBOV genomic sequences were aligned using MUSCLE.[7] Maximum likelihood was used to infer phylogeny among the two species of Ebola virus found in DR Congo, Zaire and Bundibugyo, using GARLI (v2.01) with the general time-reversible nucleotide substitution model with discrete γ distribution justified by jMODELTEST with Akaike information criterion.[8] For analysis of the Zaire EBOV, a Bayesian coalescent phylogenetic analysis was used to infer a molecular clock to estimate the dates of origin. Evolutionary rates were estimated using Bayesian Markov chain Monte Carlo inference in BEAST (v.1.10.4).[9] A Hasegawa-Kishino-Yano substitution model with γ distribution was chosen along with an uncorrelated relaxed clock with log-normal distribution and a constant population size model. A final analysis was run for 500 million chain lengths and analysed by Tracer

(v.1.7.1) to achieve an effective sample size of over 200. TreeAnnotator (v.1.10.4) estimated the maximum clade credibility tree with a 10% burn-in, and FigTree (v1.4.4) was used to edit the final phylogenetic tree.

Reverse genetic rescue of infectious virus

The Makona ZsG-VP40 plasmid based on EBOV strain H.sapiens-wt/LIB/2014/Makona-201403007 (GenBank accession KP178538) was described previously.[1] The *ZsGreen* open reading frame and porcine teschovirus 2A self-cleaving peptide were cloned at the amino-terminus of VP40. Human codon-optimised genes for nucleo-protein (*NP*), *VP35*, *VP30*, and *L* (EBOV replication proteins) were cloned into pcDNA3.1. The full-length Ituri virus was based on sequence 18FHV089 (GenBank accession MK007329). This sequence in GenBank was incomplete, missing nine nucleotides at the 3′ end and seven at the 5′ end. To replace these, we used the sequence from EBOV strain H.sapiens-wt/LIB/2014/Makona-201403007, which we had previously confirmed using 3′ and 5′ rapid amplification of cDNA ends, and found the genomic ends to be conserved in Zaire EBOV. The complete Ituri virus genome was cloned behind a T7 promoter followed by a hepatitis δ virus ribozyme and T7 terminator. Briefly, infectious virus was rescued following transfection of Huh-7 cells seeded in 12-well plates with 1 μg pEBOV, 0·5 μg pC-L (or pC-L inactive), 0·5 μg pC-NP, 0·05 μg pC-VP35, 0·05 μg pC-VP30, and 1 μg of codon-optimised pC-T7. Supernatants were harvested 4 days after transfection, clarified by low speed centrifugation, and passaged twice on Huh-7 cells in 12-well plates. Recombinant viruses were sequenced by next-generation sequencing on the MiniSeq platform (Illumina, San Diego, CA, USA) and found to contain no changes after passage.

Viral assays

Huh-7 cells were seeded at 5×10^5 cells per well in a six-well plate. The following day, cells were infected at a multiplicity of infection of 0·2. Samples were taken at various time-points (0, 24, 48, 72, 96, and 144 h postinfection), and the EBOV titre in each sample was assessed by a 50% tissue culture infectious dose assay in Huh-7 cells.

Assays to measure the anti-EBOV activities of compounds were done as described previously.[10,11] Briefly, Huh-7 cells were seeded in 96-well black-walled, CellCarrier Ultra plates (PerkinElmer) at 10 000 cells per well in FluoroBrite DMEM supplemented with 1× nonessential amino acids, 1× glutamax, and 5% FCS. The next day, unless noted otherwise, two-fold serial dilutions of compounds were generated in dimethyl-sulfoxide (DMSO), and then diluted in FluoroBrite media with 10% FCS before they were added to cells, to yield a final DMSO concentration of 0·5%. 2 h after the addition of compounds, the cells were infected with EBOV reporter viruses at a multiplicity of infection of 0·2. 3 days after infection, ZsG fluorescence was measured with a BioTek Synergy H1 plate reader (BioTek Instruments, Winooski, VT, USA) with excitation at 493 nm and emission at 505 nm, 6 mm read-height, and gain of 80.

For fluorescence microscopy, Huh-7 cells were seeded, compounds were diluted and added, and cells were infected. 3 days after infection, cells were fixed with 10% formalin and nuclei were stained with NucBlue (ThermoFisher, Waltham, MA, USA). Cells were visualised

using an Operetta high-content imaging system with a 10× objective and were quantified using Harmony (v4.1; PerkinElmer, Waltham, MA, USA).

Antibody neutralisation activity was measured in Huh-7 cells. Antibodies were diluted in DMEM with an initial dilution of 1:100 and a serial four-fold dilution for eight points. A constant amount of virus, calculated for a multiplicity of infection of 0·4, was added to all antibody dilutions and allowed to incubate for 2 h at 37°C, then added to Huh-7 cells seeded the day before at 10 000 cells per well in 96-well black-walled, CellCarrier Ultra plates. After 24 h, the medium was removed, the cells were washed with phosphate-buffered saline, and fixed in formalin. NucBlue was added to stain for nuclei and ZsG fluorescence measured per cell using an Operetta high-content imaging system with a 10× objective. Cell segmentation and ZsG intensity were quantified using Harmony (v4.1).

For compound testing, fluorescence readings from quadruplicate wells at each compound concentration were taken. Analyses of signals from antibody-inhibition experiments were done similarly, but with triplicate wells for each antibody concentration. Background signals (no virus) were deducted from fluorescence readings, and data normalised to vehicle-only control. GraphPad Prism (version 8.1.2; GraphPad Software, La Jolla, CA, USA) was used to generate concentration–response plots. A four-parameter equation was used to fit semi-log plots of the data and derive the 50% effective concentration (EC_{50}) or 50% cytotoxic concentration (CC_{50}). The selectivity index was defined as the CC_{50} divided by the EC_{50}. The data shown are from at least two independent experiments.

To test GeneXpert, virus RNA was extracted from TriPure isolation reagent (Sigma-Aldrich, St Louis, MO, USA) with Direct-zol RNA purification kits (Zymo Research, Irvine, CA, USA) and MagMax Viral RNA isolation kits (ThermoFisher). The extracted RNA was spiked into matrix and the Xpert Ebola assay was done according to manufacturer's instructions on the GeneXpert XVI system (Cepheid, Sunnyvale, CA, USA). The CDC EBOV NP and VP40 real-time RT-qPCR assays were done with SuperScript III reverse transcriptase and HiFi Platinum Taq one-step kit (ThermoFisher) in a Bio-Rad Touch CFX 96 thermal cycler (Bio-Rad, Hercules, CA, USA) for the following cycling conditions: reverse transcription at 50°C for 15 min, inactivation of reverse transcription at 95°C for 2 min, 40 cycles of 95°C for 30 s to denature, and 55°C for 60 s for annealing and probe detection.

Statistical analysis

The highest posterior density interval with 95% of the probability of the posterior distribution is reported for the Bayesian analysis of genetic sequence data by the BEAST program. The number of independent samples from the posterior distribution was estimated in the effective sample size in Tracer. The maximum clade credibility tree was calculated from the posterior sample with the maximum product of posterior probabilities of each clade in TreeAnnotator.

Statistical significance was determined using the Holm-Sidak method with $\alpha=0{\cdot}05$ for the means of each virus titre each timepoint after infection. To calculate the IC_{50}, we did a non-linear regression analysis with a variable slope and four parameters. The means of the

IC_{50}s were calculated for at least two independent experiments and the standard deviations reported.

Role of the funding source

The sponsor of the study had no role in study design, data collection, data analysis, data interpretation, or writing of the report. The corresponding authors had full access to all the data in the study and had final responsibility for the decision to submit for publication.

Results

We did a phylogenetic analysis of whole-genome sequences from each EBOV outbreak (figure 1); EBOV established four clades. Clade 1 includes viruses from the first identified EBOV outbreak in 1976–77 in the remote villages of Yambuku and Bonduni, north of the Congo River (figure 1).[12] Clade 4 includes the Makona variant viruses from the 2013–16 west African epidemic in Guinea, Liberia, and Sierra Leone. A simultaneous EBOV outbreak also occurred in 2014 in Boende (Tshuapa Province, Democratic Republic of the Congo), but these viruses are phylogenetically distinct, forming part of clade 3. EBOV from the 2018 outbreak in Bikoro (Democratic Republic of the Congo) was also in clade 3. The sequences from the current Ituri-North Kivu outbreak establish a distinct clade 2, along with viruses from a small outbreak in the northern health zone of Likati in DR Congo from 2017.

We generated plasmid DNA corresponding to an EBOV-Ituri sequence and included the *ZsGreen* reporter gene (Figure 2A; appendix p 3). Under biosafety level 4 containment, we rescued a recombinant, infectious EBOV-Ituri reporter virus. We compared the replication of EBOV-Ituri and EBOV-Makona (similarly engineered to express ZsG) in Huh-7 cells (Figure 2). The yields of EBOV-Ituri were marginally but significantly lower than those of EBOV-Makona at early time-points, and increased seven-fold between 24 h and 48 h. At 24 h post-infection the mean yield was $4{\cdot}64 \times 10^4$ 50% tissue culture infectious dose ($TCID_{50}$; SD 0) for EBOV-Makona and $3{\cdot}21 \times 105$ $TCID_{50}$ ($7{\cdot}425 \times 10^4$) for EBOV-Ituri (p=0·96), and at 48 h post-infection the mean yield was $3{\cdot}75 \times 10^6$ $TCID_{50}$ (0) for EBOV-Makona and $2{\cdot}56 \times 107$ $TCID_{50}$ ($8{\cdot}56 \times 10^6$) for EBOV-Ituri (p=0·00068). At 72 h and later, virus yields reached similar mean yields of 3×10^7 $TCID_{50}$. In addition, ZsG was readily detected when expressed by EBOV-Ituri and could be used as a reporter for screening of antiviral inhibitors (appendix p 3).

EBOV-Ituri and EBOV-Makona were equally sensitive to inhibition by remdesivir, with mean EC_{50} values of 13 nM (SD 2) for EBOV-Ituri and 12 nM (2) for EBOV-Makona (table 1; appendix p 3). Mean CC_{50} values were 3·6 μM (SD 2·9) with a selectivity index of around 300 for both viruses, consistent with previous findings (table 1).[13,14] We also tested a panel of compounds previously reported to inhibit EBOV for their ability to inhibit EBOV-Ituri. Inhibition of infection by most compounds, including ribavirin, the selective oestrogen receptor modulator inhibitors toremifene and tamoxifen, and the calcium channel blocker verapamil was similar for EBOV-Ituri and EBOV-Makona (table 1). The anti-arrhythmic drug amiodarone hydrochloride, was previously shown to block EBOV entry in vitro and was given to patients in west Africa,[15-17] but its clinical benefits remain unclear. We found

that inhibition of infection by amiodarone hydrochloride was similar for EBOV-Ituri and EBOV-Makona (table 1).

Within Zaire EBOV species, there is conservation of the GP amino acid sequence with only 31 differences between EBOV Ituri, Bikoro, Makona, and Mayinga, despite their isolations spanning 42 years (appendix p 4). However, there is greater diversity between EBOV species, which might limit the activity of EBOV monoclonal antibodies. We found that antibodies KZ52, 4G7, and 2G4 could inhibit both EBOV-Ituri and EBOV-Makona in a concentration-dependent manner. The ZMapp monoclonal antibody cocktail is composed of 2G4, 4G7, and 13C6; earlier versions contained mAbs 6D8 and 13F6.[18] KZ52 is considered the prototypical monoclonal antibody isolated from a patient in the 1995 Kikwit outbreak. The monoclonal antibodies 13C6, 6D8, and 13F6 do not inhibit either EBOV-Ituri or EBOV-Makona; these glycan cap and mucin binding antibodies have been shown to protect non-human primates from Ebola virus disease, but do not neutralise EBOV in cell culture (table 2; appendix pp 4-6).[19]

EBOV-Ituri and EBOV-Makona were also similarly susceptible to inhibition by EBOV patient monoclonal antibodies 5.6.1A2, 9.6.3D6, and 2.1.1D5, whereas 2.1.1D7 did not neutralise either virus (table 2; appendix pp 5-6)[20]Other therapeutic antibodies being tested in the 2018 Democratic Republic of the Congo outbreak are monoclonal antibody mAb114 and antibody cocktail REGN-EB3 (comprised of R3470, R3471, and R3479 monoclonal antibodies).[19,21-23] The cocrystal structure of EBOV-Mayinga GP and mAb114 implicate contact residues in GP important for mAb114 binding; these contact residues are conserved in the EBOV-Ituri sequence (appendix p 4).[24] Convalescent sera collected at Yambuku in 1976, as well as rabbit and non-human primate control sera, similarly inhibited the EBOV-Ituri and EBOV-Makona viruses (table 2; appendix pp 5-6).

Aligning the sequences available for the Ituri-North Kivu outbreak, we found a mismatch in one of the Xpert Ebola primer-binding sites in the *NP* gene (a T in the forward primer that binds 880-902 of the *NP* gene for EBO-Makona is substituted with C in the EBOV-Ituri sequence; appendix p 7). We isolated virus RNA from the EBOV-Ituri and EBOV-Makona viruses. When viral RNA was amplified using the Xpert Ebola assay, we found that both viruses had similar cycle threshold values (table 3), indicating that this mismatch did not significantly affect detection of the EBOV-Ituri sequence.

The CDC Ebola assay approved by the US Food and Drugs Administration (FDA) for emergency use is a real-time RT-qPCR assay that detects two targets, the *NP* and *VP40* EBOV genes. Aligning the primer and probe sequences against the EBOV-Ituri sequence, we found a mismatch in the middle of the *NP2* reverse primer and in the *VP40* reverse primer close to the 3′ end, at position 654 in the *VP40* open reading frame (appendix p 7). We evaluated the CDC Ebola assays alongside a VP40 assay with a redesigned primer (654G) completely complementary to the EBOV-Ituri sequence; both assays recognised EBOV-Ituri and EBOV-Makona sequences with similar sensitivities and efficiencies over the seven-log dilution series tested (figure 3; appendix p 7).

Discussion

The current EBOV outbreak in Ituri and North Kivu Provinces in DR Congo that began in July, 2018, is now the second largest ever recorded. Response to this outbreak continues to be extremely challenging, with a precarious security situation hampering case finding, contact tracing, decontamination, and other standard response activities. INRB-USAMRIID scientists have succeeded, however, in generating EBOV sequences from samples collected from patients in the region. We did a phylogenetic analysis with the Ituri-North Kivu and other EBOV sequences from past outbreaks and, consistent with the recent report by Mbala-Kingebeni and colleagues,[4] found the Ituri viruses to be an independent introduction into the human population, unrelated to the previous Bikoro outbreak which ended just weeks before this tenth outbreak began. DR Congo is endemic for at least two species of Ebola virus: Zaire and Bundibugyo. Our analysis of the 2018 outbreaks suggests that there are at least two EBOV populations circulating separately in the virus' natural reservoir. The viruses from Bikoro in the west and Ituri in the east belong to different clades (Bikoro EBOV belongs to clade 3 and Ituri EBOV to clade 2) and they only share a distant common ancestor 39 years ago. Interestingly, for all clades, the Bayesian analysis suggests the variants of EBOV to be circulating 1–2 years before each outbreak. This is inferred from the most recent common ancestor at each node of an outbreak (figure 1). Each outbreak is thought to be a separate introduction into the human population from an unknown natural reservoir. We do not know if the host is dispersed and virus transmitted among a widespread population or if virus persists in groups of mobile hosts, which must contend with geographical features, such as rivers or mountains. There might have been multiple transmission events from the host to other intermediate species before Ebola came into contact with humans. Within the EBOV species, there is 96% nucleotide identity among the viruses sequenced from 1976 to 2018. This is remarkable conservation for a negative-sense RNA virus, since RNA viruses typically have a rapid evolutionary rate. The exceptionally low diversity of all EBOV indicates genetic bottlenecks must be continually restraining the virus genome sequence.[25]

Although sequence analysis can guide the epidemiology of an EBOV outbreak, it can be difficult to predict functional aspects of a virus variant, such as sensitivity to antivirals and antibody treatments and correlates of protection in vaccine studies. There have been no EBOV isolates available to the scientific community from the past four outbreaks in DR Congo. We rescued a recombinant, infectious EBOV based on a recent circulating virus sequence in the Ituri-North Kivu region; this is only the third variant of EBOV recovered from a molecular clone. The EBOV-Ituri virus replicated slightly more slowly than EBOV-Makona, the virus responsible for the 2013–16 west Africa outbreak. Although the difference in growth was statistically significant, this marginal difference might not be biologically relevant and we have not confirmed if this difference is seen in other cell lines. Additionally, we confirmed the sequence of virus stocks used in this study but cannot exclude the presence of minor variants below the level of detection available with the Illumina method that might affect the growth of the viral population. The GP mutation Ala82Val proposed to be associated with increased infectivity and mortality in the west Africa epidemic[26-28] is not present in the Ituri sequence. Although the Ala82Val change did

not alter pathogenicity in animal models,[29] its absence might explain the somewhat reduced replication of EBOV-Ituri relative to EBOV-Makona in cell culture.

Because of the stringent laboratory containment requirements for working with infectious EBOV, surrogate assays are often used to study small molecules and antibodies to infer anti-EBOV activities. Such assays include using minigenomes for studying viral replication and pseudotype viruses for studying cell entry, and often recapitulate what is observed with the authentic virus. However, findings from experiments using surrogate assays should be confirmed with authentic virus whenever possible. For example, the predominant GP form made by authentic virus is the secreted GP; the full-length form of GP is synthesised at lower frequency and is only expressed when the viral polymerase performs the non-templated addition of an extra adenosine. The secreted GP may bind antibodies, but is not present in pseudotype virus assays. Other assays make use of GP without a mucin-like domain or with a cleaved glycan cap, but might not accurately represent findings with an intact GP. Several investigational therapies are being tested in the current Ituri-North Kivu outbreak despite a lack of evidence for effectiveness of these therapies against the circulating virus. Here, we show that the investigational drug remdesivir and monoclonal antibodies present in the antibody cocktail ZMApp, as well as other small molecules and antibodies with therapeutic potential (humanised monoclonal antibodies, patient monoclonal antibodies, and convalescent patient sera), inhibited EBOV-Ituri similarly to the more commonly used EBOV-Makona isolate. Importantly, the humanised monoclonal antibodies present in the ZMapp cocktail blocked EBOV-Ituri and EBOV-Makona infection with a similar potency.

The Xpert Ebola assay, run on GeneXpert instruments from Cepheid, has received approval for emergency use both from WHO and FDA, and is being used extensively for diagnosis in the current outbreak. The assay uses self-contained cartridges for RNA extraction and real-time RT-qPCR on two different EBOV target genes, *NP* and *GP*. As with all assays that detect nucleic acid, sequence changes might impair assay performance, resulting in reduced sensitivity or even false-negative test results. It is therefore crucial to confirm assay performance on newly emerging outbreak sequences.

The Xpert Ebola assay contains a mismatch in one of its *NP* primer-binding sites. Despite this, Mbala-Kingebeni and colleagues[4] were able to use a panel of EBOV-Ituri samples to show that the mean difference in cycle threshold values between the NP and GP assays was similar to the mean difference previously published for EBOV-Makona samples from the 2013–16 outbreak in Sierra Leone. Consistent with these observations, we showed that the Xpert Ebola assay detects the EBOV-Ituri sequence with similar sensitivity to EBOV-Makona, over a range of dilutions. Additionally, we showed that the CDC Ebola real-time RT-qPCR assay, which has a different mismatch, also detects both viruses with similar sensitivity. The satisfactory performance of these assays, despite the changes in their respective target sequences, is encouraging for their use in detecting future virus strains, but assay performance in any future outbreak should be confirmed using sequences specific to that outbreak.

One limitation of our study is that to facilitate the quantification of infection, we compared EBOV-Ituri and EBOV-Makona viruses encoding the fluorescent reporter protein ZsG. The inclusion of the *ZsGreen* gene means that these viruses are not ideal for testing in animal models to compare pathogenicity, for example, where it would be preferable to use viruses without an exogenous gene. Work to generate such a full-length EBOV-Ituri virus is underway. Additionally, although it seems unlikely, we cannot exclude the possibility that the inclusion of the *ZsGreen* gene might affect the growth of EBOV-Makona or EBOV-Ituri differently, which could affect the comparison of their growth kinetics.

Our results could help to inform outbreak response activities. Our data support the continued testing of remdesivir and ZMapp in DR Congo. We suggest that other investigational therapies such as monoclonal antibodies mAb114 and REGN-EB3 also be tested against the EBOV-Ituri strain as soon as possible, to provide a rational basis for their continued administration. We also show the validity of using authentic virus to test the performance of current diagnostic assays, and empirically prove the effect a primer mismatch might have on the efficiency of the assay.

Our work further shows the utility of viral genome sequencing during an outbreak. Such sequences could be used to supplement traditional epidemiological measures, identify chains of transmission, and help contact tracing. They could also be used to detect any known viral variants resistant to therapy and potential signatures of host adaptation. As technology progresses and rapid sequencing of virus strains in low-resource settings in the field becomes more and more feasible, if isolates are unavailable, we recommend a policy whereby reverse genetics is used to generate outbreak strains as a standard practice. As we have shown in this study, such recombinant viruses can be used to confirm the efficacy of investigational therapies and the sensitivity of diagnostic assays for use in the field. This testing might provide a rationale for the prioritisation of candidate therapeutics and could identify issues with diagnostic assays that are rectifiable by altering primer sequences.

Supplementary Material

Refer to Web version on PubMed Central for supplementary material.

Acknowledgments

This study was funded by the US Centers for Disease Control and Prevention. We thank all those involved in responding to the current EBOV outbreak in DR Congo, particularly the INRB and USAMRIID scientists without whose work to generate sequences from the current outbreak and provide them to the global public health community, this manuscript would not be possible. We thank Carl Davis and Rafi Ahmed (Emory University, Atlanta, GA, USA) for providing patient monoclonal antibodies, and Robert Jordan and Tomas Cihlar (Gilead Sciences, Foster City, CA, USA) for providing remdesivir. We thank Tanya Klimova for expert assistance in editing this manuscript. The findings and conclusions in this report are those of the authors and do not necessarily represent the official position of the Centers for Disease Control and Prevention.

Data sharing

All relevant data are available from the corresponding author upon request.

References

1. Feldmann H, Geisbert TW. Ebola haemorrhagic fever. Lancet 2011; 377: 849–62. [PubMed: 21084112]
2. WHO. Ebola situation reports: Democratic Republic of the Congo. World Health Organisation. https://www.who.int/ebola/situation-reports/drc-2018/en/ (accessed Feb 25, 2019).
3. Tchesnokov EP, Feng JY, Porter DP, Götte M. Mechanism of inhibition of Ebola virus RNA-dependent RNA polymerase by remdesivir. Viruses 2019; 11: pii E326.
4. Mbala-Kingebeni P, Aziza A, Di Paola N, et al. Medical countermeasures during the 2018 Ebola virus disease outbreak in the North Kivu and Ituri Provinces of the Democratic Republic of the Congo: a rapid genomic assessment. Lancet Infect Dis 2019; 19: 648–57. [PubMed: 31000464]
5. Kuhn JH, Bao Y, Bavari S, et al. Virus nomenclature below the species level: a standardized nomenclature for laboratory animal-adapted strains and variants of viruses assigned to the family Filoviridae The previously developed template for natural filovirus. Arch Virol 2013; 158: 1425–32. [PubMed: 23358612]
6. Albariño CG, Wiggleton Guerrero L, Lo MK, Nichol ST, Towner JS. Development of a reverse genetics system to generate a recombinant Ebola virus Makona expressing a green fluorescent protein. Virology 2015; 484: 259–64. [PubMed: 26122472]
7. Edgar RC. MUSCLE: multiple sequence alignment with high accuracy and high throughput. Nucleic Acids Res 2004; 32: 1792–97. [PubMed: 15034147]
8. Zwickl DJ. Genetic algorithm approaches for the phylogenetic analysis of large biological sequence datasets under the maximum likelihood criterion. PhD thesis, University of Texas at Austin, 2006.
9. Suchard MA, Lemey P, Baele G, Ayres DL, Drummond AJ, Rambaut A. Bayesian phylogenetic and phylodynamic data integration using BEAST 1.10. Virus Evol 2018; 4: 1–5.
10. McMullan LK, Flint M, Dyall J, et al. The lipid moiety of brincidofovir is required for in vitro antiviral activity against Ebola virus. Antiviral Res 2016; 125: 71–78. [PubMed: 26526586]
11. Mohr EL, McMullan LK, Lo MK, et al. Inhibitors of cellular kinases with broad-spectrum antiviral activity for hemorrhagic fever viruses. Antiviral Res 2015; 120: 40–7. [PubMed: 25986249]
12. Breman JG, Heymann DL, Lloyd G, et al. Discovery and description of Ebola Zaire virus in 1976 and relevance to the west African epidemic during 2013–2016. J Infect Dis 2016; 214 (suppl 3): S93–101. [PubMed: 27357339]
13. Warren TK, Jordan R, Lo MK, et al. Therapeutic efficacy of the small molecule GS-5734 against Ebola virus in rhesus monkeys. Nature 2016; 531: 381–85. [PubMed: 26934220]
14. Lo MK, Jordan R, Arvey A, et al. GS-5734 and its parent nucleoside analog inhibit filo-, pneumo- and paramyxoviruses. Sci Rep 2017; 7: 43395. [PubMed: 28262699]
15. Johansen LM, Brannan JM, Delos SE, et al. FDA-approved selective estrogen receptor modulators inhibit Ebola virus infection. Sci Transl Med 2013; 5: 190ra79.
16. Johansen LM, DeWald LE, Shoemaker CJ, et al. A screen of approved drugs and molecular probes identifies therapeutics with anti-Ebola virus activity. Sci Transl Med 2015; 7: 290ra89.
17. Gehring G, Rohrmann K, Atenchong N, et al. The clinically approved drugs amiodarone, dronedarone and verapamil inhibit filovirus cell entry. J Antimicrob Chemother 2014; 69: 2123–31. [PubMed: 24710028]
18. Davidson E, Bryan C, Fong RH, et al. Mechanism of binding to Ebola virus glycoprotein by the ZMapp, ZMAb, and MB-003 cocktail antibodies. J Virol 2015; 89: 10982–92. [PubMed: 26311869]
19. Saphire EO, Schendel SL, Gunn BM, Milligan JC, Alter G. Antibody-mediated protection against Ebola virus. Nat Immunol 2018; 19: 1169–78. [PubMed: 30333617]
20. Davis CW, Jackson KJL, McElroy AK, et al. Longitudinal analysis of the human B cell response to Ebola virus infection. Cell 2019; 177: 1–17. [PubMed: 30901532]
21. WHO. Notes for the record: Consultation on Monitored Emergency Use of Unregistered and Investigational Interventions (MEURI) for Ebola Virus Disease (EVD). Geneva: World Health Organization, June 30, 2018. https://www.who.int/ebola/drc-2018/notes-for-the-record-meuri-ebola.pdf (accessed July 1, 2019).

22. Sivapalasingam S, Kamal M, Slim R, et al. Safety, pharmacokinetics, and immunogenicity of a co-formulated cocktail of three human monoclonal antibodies targeting Ebola virus glycoprotein in healthy adults: a randomised, first-in-human phase 1 study. Lancet Infect Dis 2018; 18: 88–93.
23. Corti D, Misasi J, Mulangu S, et al. Protective monotherapy against lethal Ebola virus infection by a potently neutralizing antibody. Science 2016; 351: 1339–42. [PubMed: 26917593]
24. Misasi J, Gilman MSA, Kanekiyo M, et al. Structural and molecular basis for Ebola virus neutralization by protective human antibodies. Science 2016; 351: 1343–36. [PubMed: 26917592]
25. Carroll SA, Towner JS, Sealy TK, et al. Molecular evolution of viruses of the family filoviridae based on 97 whole-genome sequences. J Virol 2013; 87: 2608–16. [PubMed: 23255795]
26. Diehl WE, Lin AE, Grubaugh ND, et al. Ebola virus glycoprotein with increased infectivity dominated the 2013–2016 epidemic. Cell 2016; 167: 1088–98.e6. [PubMed: 27814506]
27. Urbanowicz RA, McClure CP, Sakuntabhai A, et al. Human adaptation of Ebola virus during the west African outbreak. Cell 2016; 167: 1079–87e5. [PubMed: 27814505]
28. Dietzel E, Schudt G, Krähling V, Matrosovich M, Becker S. Functional characterization of adaptive mutations during the west African Ebola virus outbreak. J Virol 2017; 91: e01913–16. [PubMed: 27847361]
29. Marzi A, Chadinah S, Haddock E, et al. Recently identified mutations in the Ebola virus-Makona genome do not alter pathogenicity in animal models. Cell Rep 2018; 23: 1806–16. [PubMed: 29742435]

Research in context

Evidence before this study

We searched PubMed using the terms “ebola” or “filovirus” combined with “DRC” or “outbreak” for articles published up to April 14, 2019, with no restrictions on language or publication date. Reports were mostly commentaries and focused on the socioeconomic aspects of the outbreak in the Democratic Republic of the Congo, particularly the difficulties with community engagement, public trust for participating in contact tracing, vaccination, and reporting to Ebola treatment centres. We found no research articles reporting the sensitivity of the Ituri-North Kivu Ebola virus to experimental therapies and its detection by diagnostic assays used in the current outbreak. After we had submitted our manuscript, two articles were released in *The Lancet Infectious Diseases* describing the Ebola virus sequences obtained from both the Equateur Province and Ituri-North Kivu 2018 outbreaks in DR Congo. Mbala-Kingebeni and colleagues sequenced Ebola virus locally and used the results to track transmission and test deployed diagnostics and medical countermeasures in silico.

Added value of this study

Ebola virus vaccines, therapeutics, and diagnostic assays have been developed on the basis of strains from past outbreaks. Using our reverse genetics system and Ebola virus sequences provided by organisations in DR Congo, we generated an authentic Ebola virus from the ongoing outbreak in Ituri and North Kivu provinces. We offer evidence that the Ebola-Ituri virus is phylogenetically distinct from past outbreak viruses, is inhibited by experimental antiviral compounds and monoclonal antibodies being tested in DR Congo, and can be detected by diagnostic assays used in the field.

Implications of all the available evidence

Our data support the continued testing of remdesivir and ZMapp in DR Congo. Our work illustrates the utility of reverse-genetic systems to generate outbreak strains, allowing the testing of investigational therapies and diagnostic assays against emerging virus sequences to provide a rational basis for response activities that may have otherwise been absent.

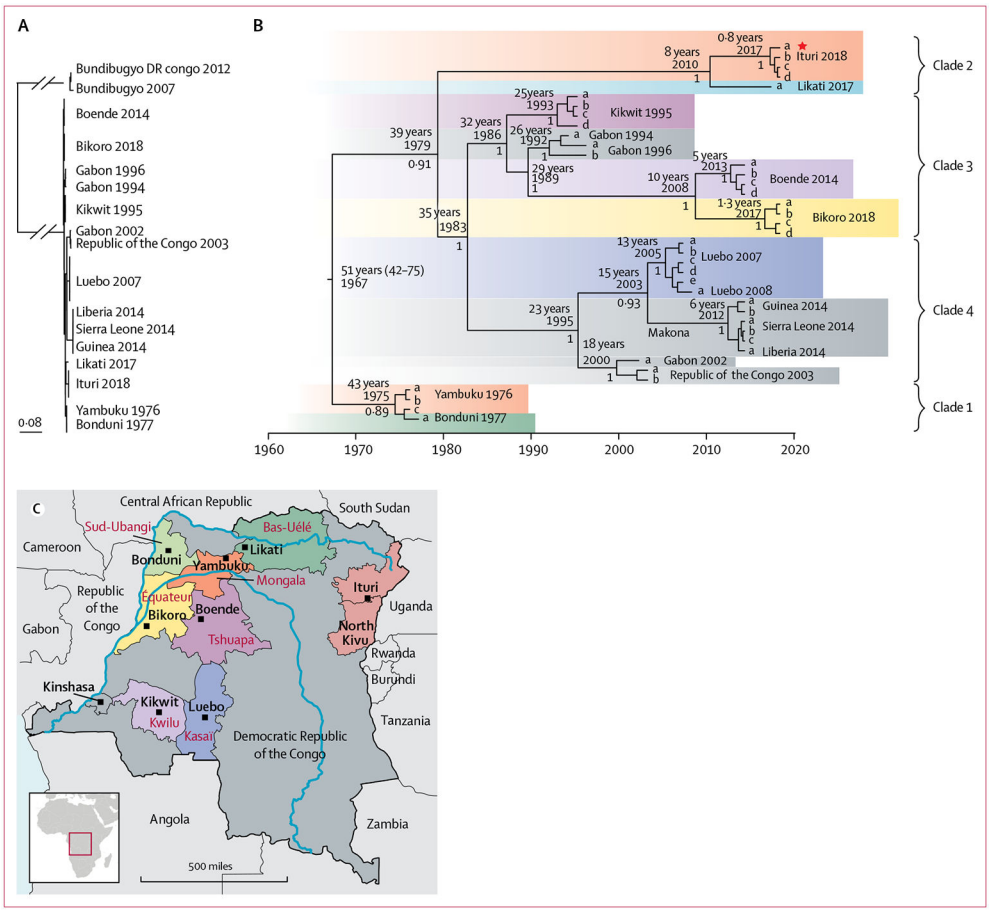

Figure 1: Phylogenetic analysis of representative complete Ebola virus genomic sequences

Bayesian coalescent phylogenetic analysis with Markov chain Monte Carlo sampling was used to infer a molecular clock to estimate the dates of origin. (A) Maximum-likelihood analysis of full-length genomes showing Ebola virus sequences cluster separately from Bundibugyo virus. Scale bar is substitutions per site. (B) Maximum clade credibility tree of the Bayesian analysis of the Ebola-Ituri sequence with those from other Ebola virus outbreaks. The most recent common ancestor, with years since 2018, and posterior probability values are shown at the nodes, and the 95% highest posterior density interval is shown in parentheses. The evolutionary rate was estimated to be $4{\cdot}6 \times 10^{-4}$ nucleotide substitutions per site per year ($2{\cdot}8 \times 10^{-4}$ – $6{\cdot}3 \times 10^{-4}$ highest posterior density), typical for an RNA virus with a 19 kb genome. The Ebola-Ituri genome used in this study is marked with a star. (C) Locations of Ebola virus outbreaks within the Democratic Republic of the Congo.

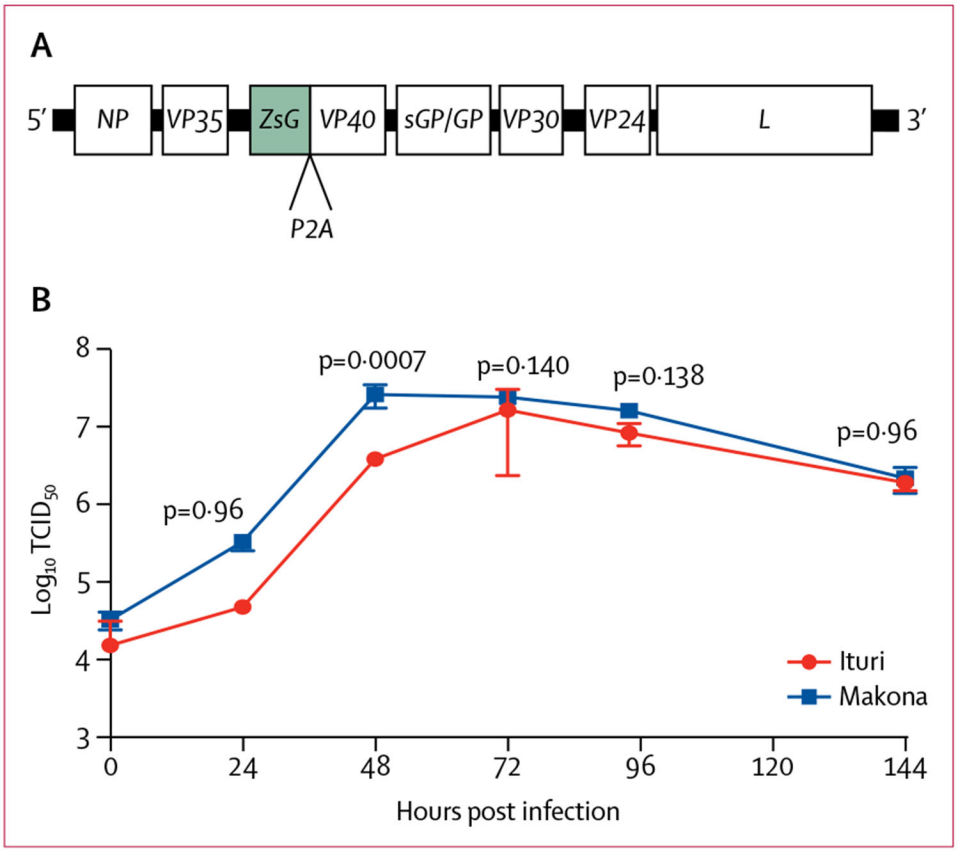

Figure 2: Recombinant EBOV-Ituri genome and replication kinetics of EBOV-Ituri and EBOV-Makona in cell culture

(A) Schematic of the recombinant EBOV-Ituri genome in viral complementary sense with reporter *ZsG* expressed with the gene for virus membrane protein *VP40* and separated by the gene for the self-cleaving *2A* peptide. (B) Time course of viral growth. Huh-7 cells were infected at a multiplicity of infection of 0·2. Samples of media were harvested at varying time points and virus titres were measured. Data represent the mean of three biological replicates and the error bars represent the SD. EBOV=Ebola virus. $TCID_{50}$=50% tissue culture infectious dose.

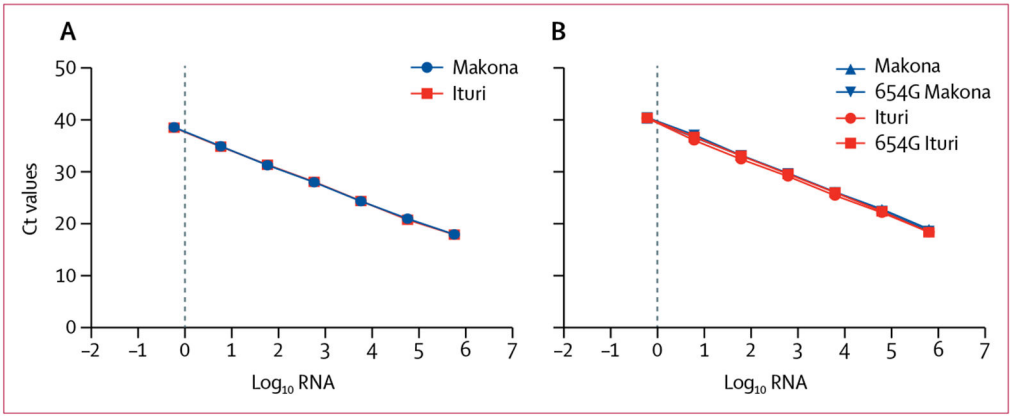

Figure 3: Performance of diagnostic assays on the Ebola-Ituri sequence

(A) Results from the CDC NP2 real-time RT-qPCR assay, using dilution series of Ituri or Makona Ebola virus RNA. (B) Results from the CDC VP40 real-time RT-qPCR assay and the modified VP40 assay that accounts for the mismatch in the *NP2* reverse primer (654G), using dilution series of Ituri or Makona Ebola virus RNA. For each assay, a representative of at least three independent experiments is shown. CDC=US Centers for Disease Control and Prevention.

Table 1:

Antiviral activities of miscellaneous compounds against Ituri-EBOV

	Comment	CC_{50} (μM)	EBOV-Makona		EBOV-Ituri	
			EC_{50} (μM)	Selectivity index	EC_{50} (μM)	Selectivity index
Remdesivir	Nucleotide analogue prodrug	3·63 (2·88)	0·012 (0·002)	303	0·013 (0·002)	279
2′-deoxy-2′-fluorocytidine	Nucleoside analogue	>50	3·15 (0·95)	>16	3·54 (1·17)	>14
Ribavirin	Guanosine analogue	>50	12·0 (3·05)	>4	17·5 (10·2)	>3
AR-12	Also known as OSU-03012	3·67 (0·14)	0·40 (0·13)	9	0·336 (0·069)	11
Azauridine	Inhibitor of pyrimidine biosynthesis	>50	50·26 (38·18)	1	34·13 (21·16)	2
Mycophenolate mofetil	Inhibitor of inosine monophosphate dehydrogenase	14·2 (4·3)	0·147 (0·093)	97	0·160 (0·082)	89
Verapamil	Calcium channel blocker	>50	41·23 (21·68)	>1	23·43 (21·36)	>2
Clomifene citrate	Selective oestrogen receptor modulator	8·43 (1·08)	0·20 (0·07)	42	0·121 (0·088)	70
Toremifene citrate	Selective oestrogen receptor modulator that blocks entry and, binds pocket on glycoprotein	>50	0·20 (0·064)	>250	0·080 (0·072)	>625
Terifluonamide	Pyrimidine de novo synthesis inhibitor	>50	7·03 (3·06)	>7	6·794 (2·681)	>7
Amiodarone hydrochloride	Antiarrhythmic agent and calcium channel blocker	13·89 (1·91)	0·904 (0·395)	15	0·563 (0·286)	25
Tamoxifen	Selective oestrogen receptor modulator	16·29 (12·05)	0·311 (0·107)	52	0·108 (0·060)	151

Data are n or mean (SD), where n is the selectivity index. The mean was calculated from at least two independent determinations. The selectivity index was defined as the CC_{50} divided by the EC_{50}. EBOV=Ebola virus. CC_{50}=50% cytotoxic concentration. EC_{50}=50% effective concentration.

Table 2:

Neutralisation activities of antibodies against Ituri-EBOV

	EC_{50} (μg/mL)		Epitope location
	EBOV-Makona	EBOV-Ituri	
KZ52	0·3005 (0·16)	0·3172 (0·01)	Base
2G4	0·4544 (0·15)	0·2412 (0·02)	Base
4G7	0·2005 (0·08)	0·4773 (0·01)	Base
13C6	Not neutralising	Not neutralising	Glycan cap
6D8	Not neutralising	Not neutralising	Mucin-like domain
13F6	Not neutralising	Not neutralising	Mucin-like domain
5.6.1 A2	0·1207 (0·02)	0·238 (0·02)	Internal fusion loop
9.6.3 D6	1·435 (0·05)	3·339 (0·10)	Glycan cap
5.1.10 B3	5·543 (2·78)	3·145 (0·07)	GP1 core
2.1.1 D5	9·38 (1·92)	>10	GP1 core
2.1.1 D7	>10	>10	GP1/2 interface
703200	7·885 (0·703)	2·832 (0·163)	NA (EBOV human convalescent Jan, 1977)
703201	2·996 (0·264)	3·75 (0·176)	NA (EBOV human convalescent Nov, 1976)
703371	0·927 (0·06)	1·207 (0·04)	NA (rabbit)
703547	1·455 (0·08)	1·957 (0·05)	NA (non-human primate)

Data are mean (SD) from at least two independent determinations.

EC_{50}=50% effective concentration. EBOV=Ebola virus. GP=glycoprotein.

NA=not applicable.

Table 3:

Comparison of cycle thresholds obtained on the Xpert Ebola assay with dilution series of Ituri and Makona Ebola virus RNA in 50% tissue culture infectious doses

	Ituri cycle thresholds		Makona cycle thresholds	
	Nucleoprotein	**Glycoprotein**	**Nucleoprotein**	**Glycoprotein**
300 000	22	30	22	30
30 000	26	34	26	34
3000	29	38	29	37
300	33	42	33	42
30	36	ND	38	ND
3	38	ND	40	ND

ND=not detected beyond the maximum cycle threshold value of 40.